Mon. Not. R. Astron. Soc. **000**, 1–9 (2005) Printed 2 February 2008 (MN LATEX style file v2.2)

Tentative detection of warm intervening gas towards PKS 0548-322 with XMM-Newton⋆

X. Barcons[1]†, F. B. S. Paerels[2], F.J. Carrera[1], M.T. Ceballos [1], M.Sako[3]
[1] *Instituto Física de Cantabria (CSIC-UC), 39005 Santander, Spain*
[2] *Columbia Astrophysics Laboratory, Columbia University, 538W, 120th Street, New York NY 10027, USA*
[3] *Stanford Linear Accelerator Center, 2575 Sand Hill Road M/S 29, Menlo Park, CA 94025, USA*

arXiv:astro-ph/0503181v1 8 Mar 2005

28 February 2005

ABSTRACT
We present the results of a long (~ 93 ksec) *XMM-Newton* observation of the bright BL-Lac object PKS 0548-322 ($z = 0.069$). Our *Reflection Grating Spectrometer* (RGS) spectrum shows a single absorption feature at an observed wavelength $\lambda = 23.33 \pm 0.01$ Å which we interpret as OVI Kα absorption at $z = 0.058$, i.e., $\sim 3000\,\mathrm{km\,s^{-1}}$ from the background object. The observed equivalent width of the absorption line ~ 30mÅ, coupled with the lack of the corresponding absorption edge in the EPIC pn data, implies a column density $N_{\rm OVI} \sim 2\times10^{16}\,\mathrm{cm^{-2}}$ and turbulence with a Doppler velocity parameter $b > 100\,\mathrm{km\,s^{-1}}$. Within the limitations of our RGS spectrum, no OVII or OV Kα absorption are detected. Under the assumption of ionisation equilibrium by both collisions and the extragalactic background, this is only marginally consistent if the gas temperature is $\sim 2.5 \times 10^5$ K, with significantly lower or higher values being excluded by our limits on OV or OVII. If confirmed, this would be the first X-ray detection of a large amount of intervening warm absorbing gas through OVI absorption. The existence of such a high column density absorber, much stronger than any previously detected one in OVI, would place stringent constraints on the large-scale distribution of baryonic gas in the Universe.

Key words: galaxies: active, X-rays: galaxies, techniques: spectroscopic.

1 INTRODUCTION

Current cosmological models restrict the baryon fraction in the Universe to a few per cent of its total matter and energy content. A large fraction of that amount of atoms, ions and electrons is strongly suspected to reside in the intergalactic medium. Lyman α clouds (including Damped Lyman α absorption systems) are seen to dominate the baryon content of the Universe at high redshift (Storrie-Lombardi & Wolfe 2000), but at lower redshifts their number density and the subsequent contribution to the ordinary matter content of the Universe decrease.

Detailed simulations of the cosmological evolution of the baryons invariably show that the Lyman α absorbing gas at temperatures $\sim 10^4$ K undergoes shock heating at lower redshifts and its temperature rises to $10^5 - 10^7$ K (Cen & Ostriker 1999; Cen et al 2001; Fang & Canizares 2000; Davé et al 2001). The baryons in the warm and hot intergalactic medium (WHIM) reach 40-60 per cent of the total baryon budget in the local universe, according to above simulations. Indeed, most of these WHIM baryons live in small sparse concentrations, and only those in the deepest potential wells (groups and clusters of galaxies) can be seen through their X-ray emission. For the remaining of the WHIM, resonance absorption lines from highly ionized elements (OVI, OVII, OVIII, NeIX, etc.) are the best chance to detect them (Hellsten et al 1998; Fang & Canizares 2000).

Tenuous gas is best detected by absorption rather than by emission, if a bright (and featureless) enough source can be found, typically an AGN. The limiting equivalent width detectable for a resonance absorption line is ultimately determined by the spectral resolution of the spectrograph in use (assuming proper channel over-sampling of each resolution element) but most often limited by the signal to noise ratio. Very roughly, for a typical $S/N \sim 10$ spectrum, where each spectral resolution element is sampled by a few channels, the weakest absorption line detectable has an equivalent width of the order of the width of one channel. For the Reflection Grating Spectrometer - RGS (den Herder et al. 2001) that we use in this paper, the spectral resolution of the first order spectra is around 60 mÅ, and therefore with

⋆ Based on observations obtained with *XMM-Newton*, an ESA science mission with instruments and contributions directly funded by ESA member states and the USA (NASA).
† E-mail: barcons@ifca.unican.es

a good quality spectrum we might hope to detect lines as weak as $10-20\,$mÅ. With the slightly higher spectral resolution grating spectrographs on *Chandra*, lines as weak as $5-10\,$mÅ can be detected, given sufficient signal to noise.

In the recent years there have been a number of detections of resonance absorption lines arising in the WHIM, both in the soft X-ray band (with *Chandra* and *XMM-Newton*) and in the Far-Ultraviolet band (with *FUSE*). A local component of the WHIM was first discovered by Nicastro et al. (2002) using *Chandra* and *FUSE* data towards PKS 2155-204. Rasmussen, Kahn & Paerels (2003) reported on the discovery of local OVII absorption towards PKS 2155-204, 3C273 and Mkn 421 with *XMM-Newton*. Fang et al (2003) confirmed the detection of a $z=0$ OVII Kα line towards 3C273 with *Chandra*.

The detection of more distant intervening WHIM seen in absorption is so far very limited. Fang et al (2002) detect an OVIII Kα absorber towards PKS 2155-204 at a redshift coincident with an enhanced galaxy density in a well studied region of the sky. McKernan et al (2003) detect OVIII Kα absorption towards the radiogalaxy 3C120, which can be interpreted either as intervening gas at $z=0.0147$ or as gas ejected by 3C120 at a velocity of $\sim 5500\,\mathrm{km\,s^{-1}}$. The current status of the detection of features from the non-local WHIM has been recently compiled by Nicastro et al (2005). In that work, it is hinted that WHIM absorption lines can account for the missing baryons in the low-redshift Universe.

In this paper we present observations of the BL-Lac object PKS 0548-322 at $z=0.069$ (Fosbury & Disney 1976). Prior to that Disney (1974) had detected the presence of a group of galaxies at $z=0.04$ around this object, suggesting that PKS 0548-322 might be a cluster member. Much more recent work by Falomo, Pesce & Treves (1995) found that there is indeed a cluster (A S549) around this BL-Lac object, but at its average redshift of $z=0.069$. X-ray emission from this cluster is very complicated to detect and measure given the brightness of PKS 0548-322.

We first use the RGS spectra to search for absorption lines. The single unresolved line found is identified as OVI Kα at a redshift intermediate between that of the BL Lac and observer. We then use the EPIC pn spectrum to help constraining the column density and Doppler velocity parameter of the absorber. We conclude by examining the turbulence of the absorbing gas and its possible temperature under the assumption of ionisation equilibrium.

2 THE *XMM-NEWTON* RGS DATA

2.1 The X-ray data

PKS 0548–322 was observed by *XMM-Newton* (Jansen et al. 2001) during its 520th revolution, starting on the 11th of October of 2002, as part of the AO-2 science operations (Obsid number is 0142270101). The observation lasted for 94,500 sec. According to the analysis of the light-curves of the various X-ray instruments, the radiation environment conditions were good and with low background except for the last $\sim$ 10 ks where strong flaring appeared. The pipeline products that were delivered to us had been processed with version 5.3.3 of the *XMM-Newton* Science Analysis Software (SAS). However, all data products were reprocessed using version 6.0.0 of the SAS. In addition, the reprocessing incorporated a number of effective area corrections with respect to the earlier pipeline processed data.

Table 1. Fits to various wavelength regions with a power law absorbed by the Galactic column.

Instrument	λ range (Å)	Γ	$\chi^2/d.o.f$	N^a_{knots}
RGS1+2	$5-35$	1.74 ± 0.02	2160.26/1351	-
RGS1	$5-35$	1.74 ± 0.02	1051.40/648	-
RGS1	$5-15$	2.00 ± 0.12	196.55/131	10
RGS1	$15-35$	1.34 ± 0.05	538.07/458	20
RGS2	$5-35$	1.74 ± 0.02	1059.15/699	-
RGS2	$5-20$	1.98 ± 0.04	599.63/499	14
RGS2	$24-35$	0.98 ± 0.18	239.10/195	14

[a] Number of knots used in the spline fit

The *RGS1* and *RGS2* data were filtered for high background flare intervals, following the data analysis threads under the *XMM-Newton* SOC pages[1]. This resulted in 84,600 s of good exposure time for both spectrographs. Both spectrographs were operated in High Event Rate mode.

The spectra of order -1 and -2 of PKS 0548-322 were detected in both spectrographs. The 2nd order spectra, however, had very few counts and were ignored in this work. The resulting 1st order spectra (in bins of width around 5 mÅ in the central part of the spectra) have a variable signal to noise ratio across the spectrum, which range from virtually zero below 6Å and above 35Å to a peak value of around $\sim 4-5$ at wavelengths $\sim 15-20$Å.

The search for absorption lines in the RGS spectra, needs to start with the determination of the continuum level. In order to perform this, we have smoothed the spectra by grouping both the RGS1 and RGS2 data in bins containing at least 50 counts. The regions below 7Å and above 35Å, where the sensitivity of the RGS is very small, have been excluded from any further consideration. The determination of a good local continuum level is crucial to assess the significance of any putative absorption line, and therefore we have restricted the continuum fits to patches of the RGS spectra where the residuals do not show any large trends.

To this goal, we have fitted separately the RGS spectra at both sides of the non-functioning CCDs. The RGS1 continuum has been determined independently in the 7-12Å and 15-35Å regions, and the RGS2 continuum has been determined independently in the 7-20Å and 24-35Å. As it is customary, we have used a single power law spectrum absorbed by a Galactic column of $2.21\times10^{20}\,\mathrm{cm^{-2}}$, but in reality any smooth function could have been used. (Note that in similar optical/UV studies, splines are often used to take into account the possible presence of weak broad emission line complexes). The standard fitting routine `xspec`, version 11.2 (Arnaud 1996) was used throughout. The fitted parameters, along with the corresponding χ^2 values, are presented in table 1. It is clear that although an absorbed power law does not provide a good enough fit to the full band, this model delivers a much more acceptable fit when restricted to either side of the non-functioning CCDs in both spectrometers. We will elaborate further on the continuum fitting in Section 2.3.

[1] http://xmm.vilspa.esa.es

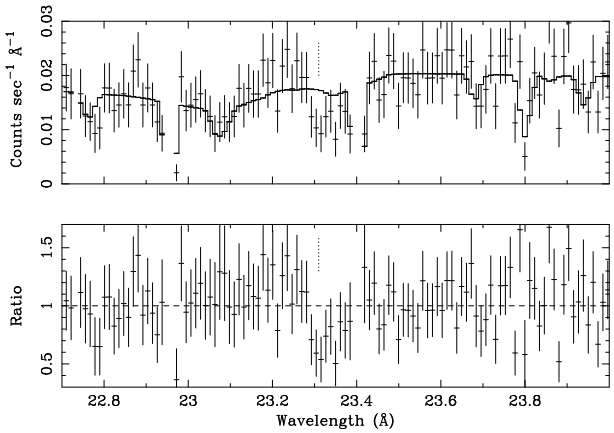

Figure 1. A portion of the RGS1 spectrum, fitted to a power law absorbed by the Galaxy, and the ratio of the data to the model. The feature at $\lambda = 23.33$ Å is the only significant feature in the whole of the RGS1 and RGS2 spectra that has a FWHM equal or larger than the spectral resolution.

2.2 Searching for absorption lines

Detecting absorption lines in a noisy spectrum is a difficult task. We have taken the ratio of the data to the continuum model fitted with the binned data, but in the original non-grouped format, to search for absorption lines. We have chosen the code EQWID, kindly provided to us by Saskia Besier at the University of New South Wales (Australia). This code searches for significant "connected" regions deviating from the continuum, knowing the spectral resolution. There are only 2 absorption features in the 4 spectral patches that have been explored, which are detected with significance above 3σ. One of them (whose centroid occurs at 26.12Å) is actually narrower (50 mÅ) than the spectral resolution of the RGS1 (60 mÅ), and is just significant at 3σ level. All this suggests that this is a non-real feature and in what follows we ignore it. There is, therefore, only one absorption line candidate detected by the EQWID software, whose centroid occurs at $\lambda = 23.33 \pm 0.014$ Å, with a FWHM of 74 ± 19 mÅ and a measured equivalent width of 32.3 ± 7.8 mÅ as returned by that code (1 sigma errors). The significance attributed to this detection is $\sim 3.7\sigma$. Unfortunately the RGS2 data does not cover that region, due to the failure of the corresponding CCD (number 4) early in the mission.

Fig. 1 shows a relevant portion of the RGS1 spectrum, where the absorption line can be seen. There is a feature in the effective area at ~ 23.35 Å which De Vries et al. (2003) attribute to an 1s-2p Oxygen transition in the instrument. This feature, which occurs at a slightly, but significantly longer wavelength. The wavelength discrepancy between the instrumental absorption feature, and the feature we detect in our source amounts to ~ 0.02 Å, or slightly more than one third of an RGS resolution element. The wavelength scale has been calibrated to much higher accuracy (8 mÅ; den Herder et al 2001). In addition, as we will show below, the measured equivalent width is significantly larger than that of the instrumental feature; and the presence of the instrumental feature is of course explicitly taken into account in the quantitative spectral analysis. We conclude that a misidentification of the feature in PKS0548-322 is excluded.

To further our confidence, we have also inspected other high signal to noise RGS spectra of extragalactic objects. Rasmussen, Kahn & Paerels (2003) present RGS spectra of 3C273, PKS 2155-304 and Mkn 421. In all 3 cases an OVII Kα absorption line at $z = 0$ (21.60 Å) is seen, with equivalent width $\sim 15 - 26$ mÅ, i.e., weaker than our detection. In these spectra, however, there are no features detected at around 23.33 Å. Section 2.3 presents a further test, based on the split of our observations in two parts, which enhances the reliability of the detected feature.

2.3 More on the continuum and significance of the absorption line

All the previous study is based on the assumption that a power law absorbed by the Galactic column fits well the RGS spectra on either side of the non-functioning CCDs and that the calibration (specifically the effective area) is accurate enough. Indeed, the spectrum of PKS 0548-422 could have slight, local deviations from the above model and the calibration could still be affected by small-scale systematics. As it has been mentioned, the way these issues are solved in optical/UV absorption line studies is by fitting a local continuum -regardless of its physical meaning-, often using splines. Visually, the continuum adopted so far around the putative feature appears a bit low, and this adds interest to this further analysis.

Therefore we have taken the data to continuum ratio resulting from the fits to either side of the non-functioning CCDs in both spectrometers and tried to fit a spline to each one individually. A region around the absorption line and the instrumental feature ranging from 23.29 Å to 23.38 Å has been masked out from this study. In order to prevent overfitting, that could eventually follow statistical noise spikes and even potential absorption or emission features, we explored the decrease of the χ^2 as a function of the number of knots adopted. We then decided to adopt a number of knots below which the χ^2 was not monotonically decreasing. This number, an obvious function of the wavelength width of the fitted region, is also shown in table 1. In all cases the spline fitting implies a substantial decrease in the χ^2 fit to a constant. The data to model ratio for the 4 spectral zones were then divided by the spline fits and this was then used for further investigation as explained in what follows.

The routine EQWID was run on the newly re-normalized ratios. Two features were found with a formal significance above 3σ. One at $\lambda = 14.70 \pm 0.02$ has a too narrow width (FWHM is only 21 mÅ) to be consistent with a real absorption line and it is therefore excluded. The other one, is the same line found without re-fitting the continuum, with the same formal significance of 3.7σ, the same central wavelength $\lambda = 23.33 \pm 0.012$, a similar width of 86 ± 19 mÅ and a slightly larger equivalent width of 39 ± 8 mÅ. This latter difference is indeed due to the fact that the continuum fitted by the splines is slightly larger. However, we decided to be conservative and keep the values presented in last subsection, bearing in mind that the highly uncertain continuum could change the equivalent width of the line probably upwards.

There is one further experiment we can do with the data to model ratio re-normalized to the continua spline fits, given the fact that the distribution of these ratios appears approx-

imately gaussian. This is to assess the real significance of the line detected, by means of Monte Carlo simulations. In order to perform this, we generated re-normalized data to model ratio spectra within the same 4 spectral bands, by assuming that values for each channel are gaussian distributed with mean 1 and dispersion given by the error bar of the data to model re-normalized ratio in the real data. Note that since the signal to noise ratio varies significantly across the spectra and therefore we cannot use an overall value for the dispersion of the gaussian.

We run 10,000 independent simulations, and on each one of them we run the EQWID software. We filtered out those features detected which have either a positive equivalent width (corresponding to an emission feature) or a width smaller than the spectrometer's resolution (60 mÅ). With these filters, a total of 605 lines were detected in the 10,000 simulations with a formal significance above 3.7σ. This in practice means that the probability of the detected feature at $\lambda = 23.33$ being a random noise feature is 6%. Indeed this implies a real significance close to 2σ. We have not, however, inspected every individual spectrum where a fictitious absorption line has been detected by EQWID, but a random inspection of a few of them shows that many do not conform to the shape of an unresolved line and Voigt profile fitting either does not converge or results in a very poor fit. This implies that the real probability that the detected feature is real is actually higher than 2σ.

2.4 Identifying and measuring the absorption line

To characterize this absorption feature, we have first modeled the absorption feature by using the *notch* model in `xspec`, added to absorbed power law. This *notch* model describes a fully saturated absorption "square" feature, which is good enough in our case as the line appears unresolved. Inclusion of this new component in the fit to the RGS1 data in the 15-35 Å range produces a decrease in the χ^2_{RGS} from 1800.17 (for 1620 degrees of freedom) to 1790.38 (for 1618 degrees of freedom). The F-test yields a significance of 98.8% to this new component, slightly smaller than the significance of the line itself, as computed by EQWID. We attribute this to the inaccurate modeling of the line by this simple model. The best fit is found at a wavelength of $\lambda = 23.33^{+0.028}_{-0.023}$ Å and an equivalent width of 32^{+23}_{-16} mÅ (90 per cent errors for one single parameter). Fig. 2 shows the best fit and confidence contours for the observed equivalent width and absorption line energy using the *notch* model, both in keV.

A further test has been performed in order to check whether an unfiltered bad event (or a set of them) in the region used to subtract the background could be responsible for the absorption feature. Note, however, that the shape of the absorption feature conforms to an approximately unresolved absorption line. To this end we splitted the RGS1 event file in two approximately equal halves in time, extracted the corresponding spectra, and computed χ^2 from the previously fitted models with and without the notch. The residuals of the model without the absorption modeled, both show a negative signal around ~ 23.33 Å. Adding the notch model, for the first half of the observation the χ^2 goes down from 1931.27 to 1926.83 when the absorption "notch" is included with the parameters fitted to the overall spectrum, and for the second half the χ^2 also decreases from 1895.56 to 1891.64. Therefore, although each half of the observation is not sensitive enough for a detection of the absorption feature, it is clear that a single bad event in the background region is not producing the observed line.

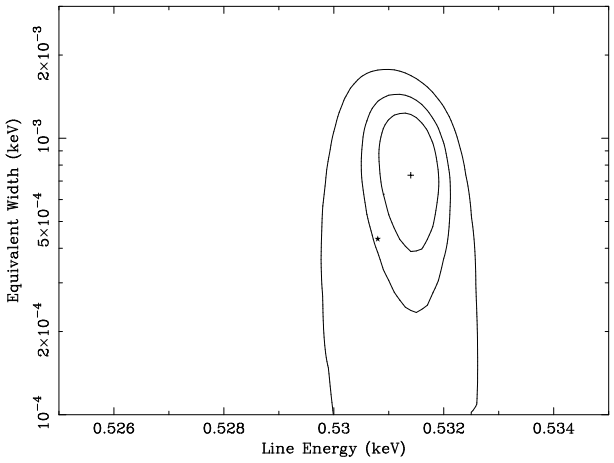

Figure 2. Best fit (+ sign) and confidence contours (1, 2 and 3 sigma) for the line energy and equivalent width of a *notch* model fitted to the absorption line. The star sign represents the instrumental feature reported by De Vries et al. (2003), which is $\sim 2\sigma$ away, and in fact already accounted for in the continuum model.

In order to identify the absorption line, assuming it is caused by intervening material, we made an extensive search for resonance lines associated to ground configurations, falling in the wavelength range from ~ 23.33 Å (in the case absorbing material occurs at $z = 0$) down to ~ 21.82 Å (in the case the line occurs at the redshift of PKS 0548-322 $z = 0.069$). Note that the most often seen Kα transition of OVII (at a rest wavelength of 21.60 Å) falls outside this range by a large amount. In fact, for the line to be identified as OVII λ21.60 the intervening material would have to be falling towards PKS 0548-322 at a velocity of $\sim 3000\,\mathrm{km\,s^{-1}}$, which is far too large for a cluster of galaxies, especially for a poor cluster like A S549. Note that a significant velocity difference (but in the opposite sense) has also been found by McKernan et al (2003) in an OVIII Kα absorber towards 3C120. In that case (but not in ours, if the line is OVII Kα) there is a possible interpretation of the absorbing gas as being in the jet and moving towards us.

The only physically meaningful option for that line is that it is OVI Kα λ22.05, which has an oscillator strength of 0.576 (Pradhan et al. 2003). There is a further line in the doublet at λ21.87, but its oscillator strength (0.061) is far too small to be detectable. Taking that interpretation, and the central wavelength measured by the notch model, the redshift of the absorbing gas is at $z = 0.058 \pm 0.001$.

Having established the nature of the line at 23.33 Å as OVI, it is natural to search for the most often seen OVII λ21.60 line. In order to do this, we model the RGS1 data by including two notches tied down at the same (free) redshift, but assuming that one is OVI λ22.05 and the other one OVII λ21.60. The fit does not improve with the inclusion of the extra notch, but then we have explored a range in parameter space to establish limits on the equivalent width of the OVII absorption line. Fig. 3 shows the results, first in equivalent width for OVI and OVII space and then for the OVI/OVII

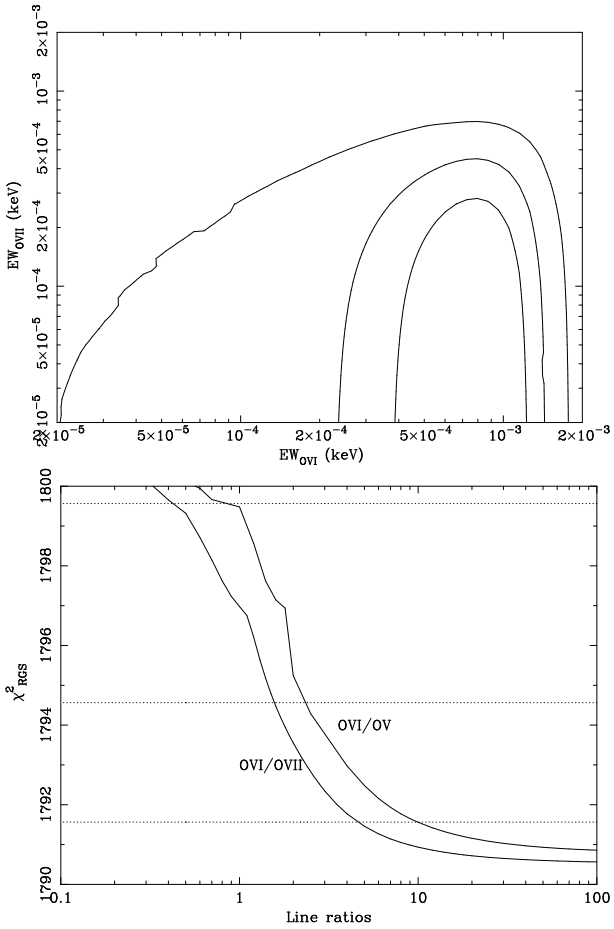

Figure 3. Top: Confidence contours in the equivalent width of OVII and OVI parameter space, as obtained by simultaneously fitting two notches at the OVI and OVII Kα wavelengths and at the same redshift. Bottom: χ^2_{RGS} (along with 1, 2 and 3 sigma confidence levels) for OVI/OVII and OVI/OV equivalent width ratios, as derived from the same data.

Table 2. Wavelength and oscillator strength of the Kα transitions for the various Oxygen ions considered here

Ion	λ (Å)	Oscillator strength
OV	22.35	0.565
OVI	22.05	0.576
OVII	21.60	0.694

equivalent width ratio. The conclusion is that OVI/OVII ratio is larger than 4.5, 1.5 and 0.4 at 1, 2 and 3 sigma confidence respectively. We have similarly constrained the equivalent width of the OV Kα line at 22.35 Å.

2.5 Profile fitting

Fig. 4 shows the curve of growth for the OVI λ22.05 transition, for a range of Doppler velocity broadening parameters b ($b = \sqrt{2}\sigma_v$, σ_v is the velocity dispersion of the gas, assumed Maxwellian). Although the range of equivalent widths allowed at 90 per cent level is large, it is clear that some level

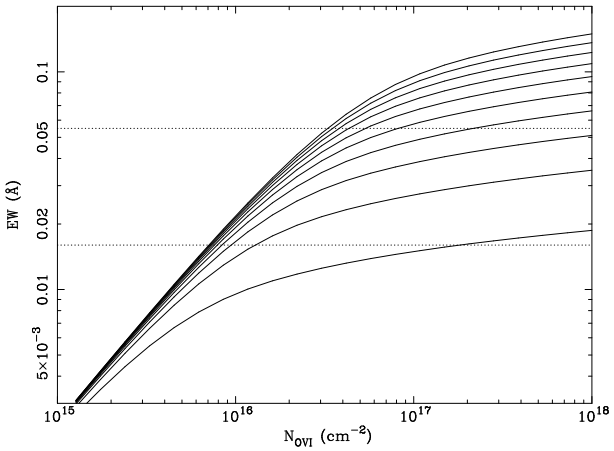

Figure 4. Curve of growth for the OVI transition at 22.05 Å. The various curves (from bottom to top) correspond to Doppler parameters b from 50 to 500 km s^{-1} in 50 km s^{-1} steps. The horizontal lines denote the 90 per cent confidence region allowed by the data.

of Doppler broadening needs to be present or otherwise the implied value of $N_{\rm OVI}$ would be very large.

To gain more insight on the physical modeling of the absorption line, we have performed a Doppler-broadened Voigt profile fitting to the ratio of the data to model in RGS1. The Voigt profile has been approximated with the formula by Whiting (1968) (accurate to better than 5 per cent), the thermal broadening is parameterized in terms of the b parameter and the spectrometer response has been modeled as a gaussian of FWHM 750 km s^{-1} outside `xspec` (i.e., the model spectrum has been convolved with that gaussian before being compared to the ratio of data to continuum). Natural broadening (both radiative and auto-ionising) is only relevant to very high column densities and it has been ignored here. Fits were restricted to the $22-24$ Å range.

Since a fit with the three parameters ($N_{\rm OVI}$, b and z) left free yielded an undefined value for b ($b = 435 \pm 420$ km s^{-1}, 1-sigma error), we fixed b to a reasonable value of 200 km s^{-1} (see later). The best fit provides a substantial improvement of the χ^2_{Voigt} which goes from 182.4 for 171 data points to 164.94 with 2 degrees of freedom less. The F-test significance of this improvement is at the level of 99.98 per cent. The best fit values are $z = 0.0580^{+0.0008}_{-0.0006}$ and $\log N_{\rm OVI}({\rm cm}^{-2}) = 16.30 \pm 0.35$ (90 per cent errors). Fig. 5 shows the portion of the spectrum fitted, where it is seen that the fit is indeed satisfactory.

There is a previous, shorter *XMM-Newton* observation of PKS 0548-322 (Obsid number 0111830201), performed on October 3, 2001. The RGS spectra (which accumulate ~ 48 ks of good exposure time each) have been presented and analyzed by Blustin et al. (2004) which do not find evidence for any significant absorption or emission features. Our own analysis of that data is entirely consistent with this. In fact, including an OVI absorption line with the parameters fixed to the above values, to the ratio of data to continuum in the 22-24Å region of the shorter exposure spectrum results in an *increase* of the χ^2 from 59.13 (for 59 degrees of freedom) to 66.73. This increase is, however, too modest to exclude the possibility that the line is present in the noisier spectrum. There is also the possibility of a transient absorption feature,

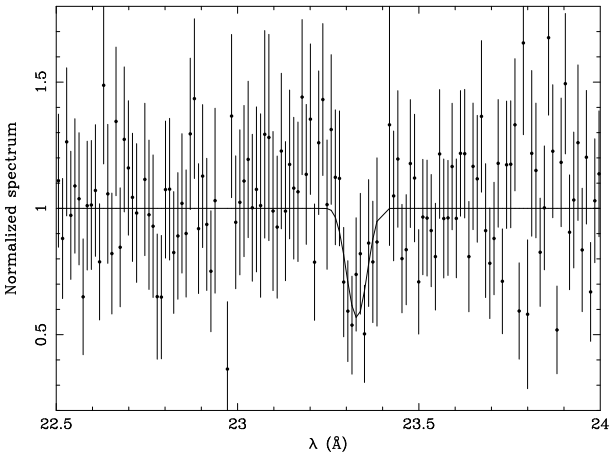

Figure 5. Fit to the ratio of the data to the continuum with a Voigt profile for the OVI line, Doppler broadened with $b = 200\,\mathrm{km\,s^{-1}}$.

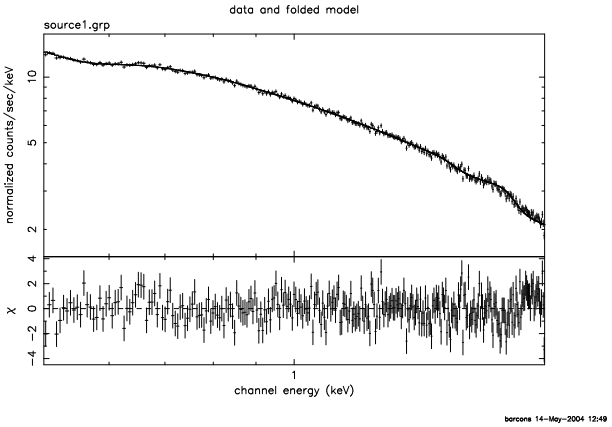

Figure 6. EPIC-pn spectrum and deviations to a power law model seen through Galactic absorption.

as discussed by Blustin et al. (2004) for broad absorption features in BL Lacs.

3 THE EPIC DATA

The two EPIC MOS detectors (Turner et al. 2001) operated in *Fast Uncompressed* mode, where the central chip (where the target was) is read as a single pixel. Since a proper background subtraction cannot be performed in this mode, we ignored the MOS data.

The EPIC pn detector (Strüder et al. 2001) was operated in Large Window mode. After filtering out high-background episodes, the net exposure time where data were extracted went down to 77.2 ks. The spectrum of the source was extracted, following the SAS analysis threads, using a circle of radius $\sim 40''$. The background spectrum was extracted from a ~ 5 times larger region free from obvious sources, although in a different CCD chip and at a different detector `y` coordinate.

The count rate from the source region is 15.42 $\mathrm{ct\,s^{-1}}$ (without any pattern filtering), slightly above of the count rate quoted in the *XMM-Newton* Users Handbook of 12 $\mathrm{ct\,s^{-1}}$ where pile-up starts to be relevant. In order to quantify the effects of pile-up, we used the SAS task *epatplot* which extracts the spectral distribution of the events with various patterns (singles, doubles, triples and quadruples) and compares that to a pile-up free model. The comparison shows that in the 0.5-2 keV is very little affected by pile-up, with an overall survival of single events of 99.2% and an overall survival of double events of 98.7% in that band. The differences between the predicted and observed spectral distributions do not exceed a few per cent at any particular channel in that band, which is of the order of the accuracy in the calibration of the EPIC-pn. We then believe that the EPIC-pn can be safely used in the 0.5-2 keV band. Above that energy, and particularly around 2-3 keV, deviations from the non-piled-up model, exceed 10-15 per cent and consequently we ignore these data.

Thence we have used the 0.5-2 keV band photons, keeping only single and double events and only those with good spectral quality (`FLAG = 0`). A fit to a power law with Galactic absorption fixed at $N_H = 2.21 \times 10^{20}\,\mathrm{cm^{-2}}$ yields a photon spectral index $\Gamma = 2.000 \pm 0.005$ (90 per cent errors). The unabsorbed flux in the 0.5-2 keV band is $S(0.5-2) = (1.865 \pm 0.004) \times 10^{-11}\,\mathrm{erg\,cm^{-2}\,s^{-1}}$.

Fig. 6 displays the spectral fit and the residuals, where there are no obvious deviations from the model (none exceeds 5 per cent at any energy in the $0.5-2$ keV). The fit is good, with $\chi^2_{pn} = 354.51$ for 302 degrees of freedom, leaving a probability that the model is wrong of only 2 per cent. Our data does not show the previously claimed presence of spectral features in this object as seen by the *Einstein Observatory* (Madejski et al 1991) and ASCA (Tashiro et al. 1994), which were tentatively interpreted as absorption edges. Such features, that were once thought to be universal among BL Lacs, are absent in the current data.

We have also tried to search explicitly for the presence of OVI in this spectrum, by using the *siabs* absorption model (Kinkhabwala et al 2003). This model keeps track of both the photoelectric absorption edge and the resonance absorption lines (modeled in terms of proper Voigt profiles) for a given ion species. Fixing the redshift of the absorber at the value measured in the RGS data ($z = 0.058$) and with a velocity dispersion corresponding to $b = 200\,\mathrm{km\,s^{-1}}$ and with the RGS best fit $N_{\rm OVI} = 10^{16.3}\,\mathrm{cm^{-2}}$ the χ^2_{pn} improves by less than one unit. Fig. 7 shows χ^2_{pn} as a function of $N_{\rm OVI}$ for the EPIC-pn data, where it can be seen that the best fit values from the RGS data are within the 1 sigma level (assuming $b \sim 200\,\mathrm{km\,s^{-1}}$).

4 PROPERTIES OF THE ABSORBING GAS

4.1 Turbulence

Since large values of $N_{\rm OVI}$ are not allowed by the EPIC-pn data, this poses additional constraints on the curve of growth for OVI. In particular, a $\sim 30\,\mathrm{m\AA}$ absorption line resulting from a large column and very little turbulence (small b-parameter) will be inconsistent with the EPIC-pn spectrum.

To quantify this, we have explored a grid of values of $N_{\rm OVI}$ from 2×10^{15} to $2 \times 10^{17}\,\mathrm{cm^{-2}}$ and for the Doppler parameter b ranging from 50 to $1000\,\mathrm{km\,s^{-1}}$. The RGS1 ratio to the continuum has been Voigt profile fitted in the range

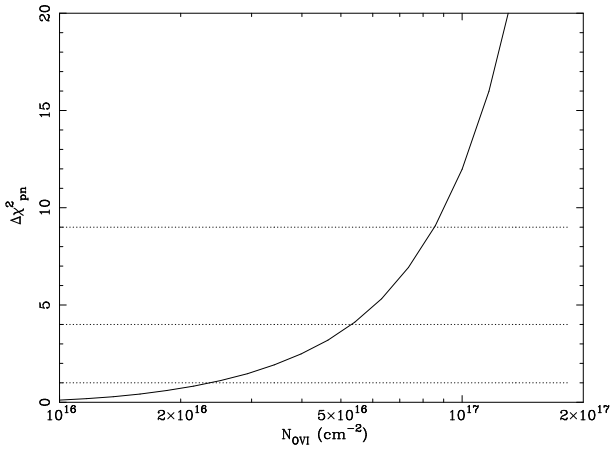

Figure 7. χ^2_{pn} (the minimum has been subtracted) as a function of the column density $N_{\rm OVI}$ for the fit to the EPIC-pn data in the 0.5-2 keV band to a power law absorbed by the Galaxy and an OVI absorber at $z = 0.058$, using the `siabs` model (Kinkhabwala et al 2003).

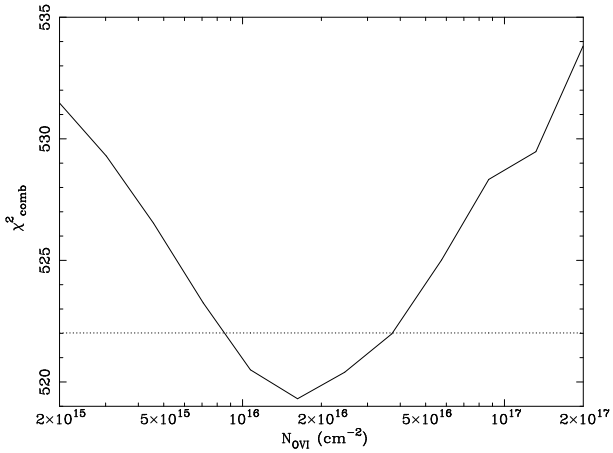

Figure 8. χ^2_{comb} as a function of OVI column density, for a joint fit to the EPIC-pn and the RGS1 ratio, where the Doppler velocity parameter b has been marginalized. The dotted line shows the 90 per cent confidence level.

22-24 Å and the EPIC-pn spectrum has been fitted in the 0.5-2 keV with a model consisting of a power law (absorbed by the Galactic H column) and a single OVI ion as defined by the model `siabs` at $z = 0.058$. For each value of the parameters $N_{\rm OVI}$ and b the line centre in the RGS1 ratio is left as a free parameter and the power law in the EPIC-pn data is also left as free (2 free parameters). We then minimise

$$\chi^2_{comb} = \chi^2_{Voigt} + \Delta\chi^2_{pn}$$

Formally the minimum χ^2_{comb} is found at $\log N_{\rm OVI}({\rm cm}^{-2}) \sim 16.3$ and $b \sim 300\,{\rm km\,s}^{-1}$. Fig. 8 shows χ^2_{comb} as a function of $N_{\rm OVI}$, coonsidering b an uninteresting parameter, from which we derive $\log N_{\rm OVI} = 16.3 \pm 0.3$ (90 per cent errors). Fig. 9 shows χ^2_{comb} as a function of b, where $N_{\rm OVI}$ has been marginalized. At 90 per cent confidence level $b = 300^{+500}_{-200}\,{\rm km\,s}^{-1}$ (i.e., $b > 100\,{\rm km\,s}^{-1}$), but what is most important, very small values of b are very unlikely. In fact $b < 50\,{\rm km\,s}^{-1}$ is excluded at $> 3\sigma$ confidence, implying that the absorbing gas is turbulent. Very large values of b cannot be excluded by this analysis because combined with smaller values of the column density they can still fit the RGS absorption line.

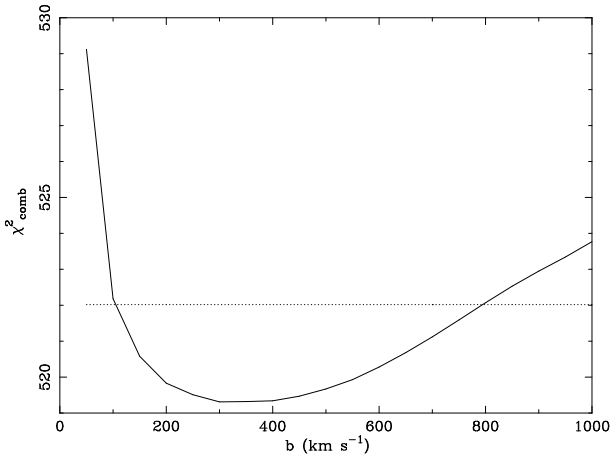

Figure 9. χ^2_{comb} as a function of Doppler velocity parameter b, for a joint fit to the EPIC-pn and the RGS1 ratio, where the OVI column density has been marginalized. The dotted line shows the 90 per cent confidence level.

4.2 Temperature

To test under what physical conditions can the observed limits on the OVI/OVII and OVI/OV line ratios take place, we performed a number of `cloudy` runs (Ferland et al. 1998). We assume an optically thin cloud of gas confined by gravity, which is ionised both collisionally and by photoionisation from the extragalactic background. We assumed the gas to be uniform, with 0.3 solar metallicity, temperature ranging from 10^4 to 10^7 K and particle density ranging from 10^{-6} to $10^{-3}\,{\rm cm}^{-3}$. The particle column density was fixed at some low but realistic value $10^{20}\,{\rm cm}^{-2}$, but line ratios are independent on this in the optically thin conditions assumed. We adopt the simple extragalactic parametrization used by Nicastro et al. (2002), as a broken power law with energy spectral indices 1.1 and 0.4 respectively below and above 0.7 keV, normalized to $10\,{\rm keV\,s}^{-1}\,{\rm cm}^{-2}\,{\rm sr}^{-1}\,{\rm keV}^{-1}$ at 1 keV (Barcons et al. 2000).

Fig. 10 shows the 1,2 and 3σ contours allowed in the density-temperature parameter space by the measured OVI/OVII and OVI/OV line ratios. Note that in displaying these contours, the line intensity ratios derived from the spectral fitting for the various Kα transitions, have been converted to column density ratios (which is what *cloudy* computes) by dividing each one by its oscillator strength (see Tab. 2). Collisional ionisation dominates at densities $> 10^{-5} - 10^{-4}\,{\rm cm}^{-3}$, but at the low density end photoionisation by the extragalactic background is the dominating ionisation process. The 3σ upper limit on the gas temperature for OVI being seen but OVII being undetected is around 2.5×10^5 K, fairly independent of the density. This same value of the temperature is also about the 3σ *lower* limit for OVI being detected but OV being undetected.

The conclusion is that it is very difficult for gas under these conditions to show only OVI Kα absorption, without OV and/or OVII absorption.

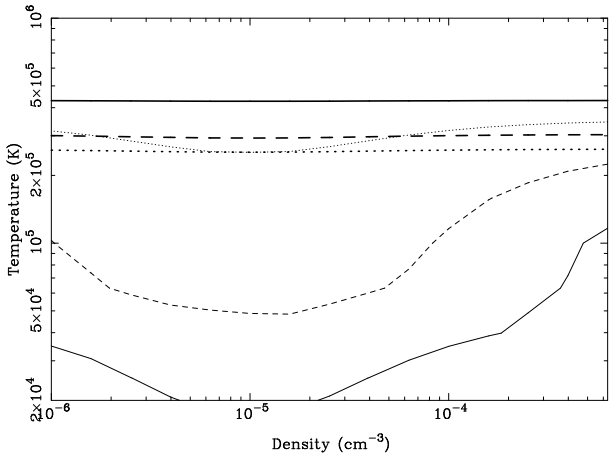

Figure 10. Region allowed in the Temperature - Density parameter space of the absorbing gas, as obtained from the constraints on the OVI/OVII (thin) and OVI/OV (thick) ratios: 1σ (solid), 2σ (dashed) and 3σ (dotted).

5 DISCUSSION

The *XMM-Newton* RGS1 spectrum of PKS 0548-322 ($z = 0.069$) shows a single absorption feature, formally significant at the 3.7σ level. Monte Carlo simulations show that this significance is probably lower, but in any case higher than 2σ. Intervening OVI Kα absorption at $z = 0.058$ is the most likely interpretation of the absorption line. The equivalent width is $\sim 30 - 40\,$mÅ, a value that is of the order of the one expected to be produced by a group or cluster. We do not find any significant absorption feature corresponding to the local WHIM ($z = 0$), nor to the putative cluster surrounding PKS 0548-322 ($z = 0.069$). Interpreting the detected absorption line in terms of OVII Kα absorption at the cluster redshift, would require the gas inflowing towards the BL Lac at a velocity close to $3000\,\mathrm{km\,s^{-1}}$, which is at odds with the expectation that BL Lacs eject material towards the observer.

Despite previous claims on the presence of strong absorption edges (Madejski et al 1991; Tashiro et al. 1994), we do not find such edges in the 0.5-2 keV EPIC-pn spectrum of PKS 0548-322. Adopting the OVI identity for the absorption feature and combining the spectral fits to the RGS1 spectrum normalized to the continuum (Voigt profile fitting) with the EPIC pn data, we find that the absorber has an OVI column of $\log N_{\rm OVI}(\mathrm{cm}^{-2}) = 16.3\pm0.3$, with significant turbulence (Doppler velocity parameter $b > 100\,\mathrm{km\,s^{-1}}$ at 90 per cent confidence). The lack of OV and OVII Kα absorption lines in the RGS1 spectrum, however, impose almost discrepant conditions to the temperature of the absorbing gas (assumed in ionisation equilibrium by collisions and the extragalactic background). Marginal consistency is only achieved if the gas has a temperature $T \sim 2.5 \times 10^5\,$K.

If confirmed this would be the first detection of absorption by X-ray gas at such a low temperature. Simulations do show that absorbing gas blobs in the WHIM should span a range of temperatures between 10^5 and $10^7\,$K (Davé et al 2001), although so far only higher ionisation species, probably corresponding to the highest temperatures in that range, have been detected. Chen et al (2003) have specifically studied the cosmological distribution of OVI absorbers via simulations. Large column density systems, such as the one tentatively detected here, are extremely rare according to the simulations. If confirmed, this would represent a strong challenge to our knowledge of the distribution of baryons in Cosmic scales.

The fact that no other features associated either to the intervening absorber itself or to the local WHIM are not detected, calls for the need of a better S/N high spectral resolution spectrum to confirm the existence of this peculiar absorber.

ACKNOWLEDGMENTS

We are grateful to S. Besier and A. Fernández-Soto for help in the Voigh profile fitting. Comments from an anonymous referee, which resulted in substantial improvement of the paper, are also appreciated. XB, FJC and MTC acknowledge partial financial support by the Spanish Ministerio de Educación y Ciencia, under project ESP2003-00812. FP acknowledges support from NASA, under grant NAG5-7737.

REFERENCES

Arnaud K.A., 1996, in Jacoby G.H., Barnes J., eds, ASP Conf. Ser. Vol 101, Astronomical Data Analysis Software and Systems V. Astron. Soc. Pac,. San Francisco, p.17
Barcons X., Mateos S., Ceballos M.T., 2000, MNRAS, 316, L13
Blustin A.J., Page M.J., Branduardi-Raymont G., 2004, A&A, 417, 61
Cen R., Ostriker J.P., 1999, ApJ, 514, 1
Cen R., Tripp T.M., Ostriker J.P., Jenkins E.B., 2001, ApJ, 559, L5
Chen, X., et al., 2003, ApJ, 594, 42
Davé R., et al, 2001, ApJ, 522, 473
de Vries, C.P., den Boggende A.J., den Herder J.W., Kaastra J.S., Paerels F.B., Rasmussen A.P., 2003, A&A, 404, 959
den Herder J.W. et al., 2001, A&A, 365, L7
Disney M.J., 1974, ApJ, 193, L103
Falomo R., Pesce J.E., Treves A., 1995, ApJ, 438, L9
Fang T., Canizares C.R., 2000, ApJ, 539, 532
Fang T., Marshall H.L., Lee J.C., Davis D.S., Canizares C.R., 2002, ApJ, 572, L127
Fang T., Sembach K.R., Canizares C.R., 2003, ApJ, 586, L49.
Ferland G.J., Korista K.T., Verner D.A., Ferguson J.W., Kingdon J.B., Verner E.M., 1998, PASP, 110, 761
Fosbury R.A.E., Disney M.J., 1976, ApJ, 207, L57
Hellsten U., Gnedin N.Y., Miralda-Escudé J., 1998, ApJ, 509, 56
Jansen F.A., et al, 2001, A&A, 365, L1
Kinkhabwala A., Behar E., Sako M., Gu M.F., Kahn S.M., Paerels F.B.S., 2003, ApJ,
Madejski G.M., Mushotzky R.F., Weaver K.A., Arnaud K.A., Megan C.M., 1991, ApJ, 370, 198
McKernan, B, Yaqoob T., Mushotzky R., George I.M., Turner T.J., 2003, ApJ, 598, L83.
Nicastro F., et al., 2002, ApJ, 573, 157
Nicastro F., et al. 2005, Ad. Sp. Res., in the press

Pradhan A.K., Chen G.X., Delhaye F., Nahar S., Oelgoetz J., 2003, MNRAS, 341, 1268

Rasmussen A., Kahn S.M., Paerels F., 2003, in: *The IGM/Galaxy Connection: The Distribution of Baryons at z=0*, ASSL Conference Proceedings Vol. 281, Edited by Rosenberg J.L. & Putman M.E., Kluwer Academic Publishers, Dordrecht, p.109

Storrie-Lombardi L.J., Wolfe A.M., 2000, ApJ, 543, 552

Strüder L., et al, 2001, A&A, 365, L18

Tashiro M., Ueda Y., Kii T., Makino F., Fujimoto R., Mushotzky R.F., Makishima K., Yamashita A., 1994, in *New Horizon of X-ray Astronomy -first results from ASCA-*, Ed. by F. Makino & T. Ohashi, Universal Academy Press, p. 343

Turner M.J.L., et al., 2001, A&A, 365, L27

Whiting E.E., 1968, J. Quant. Spectrosc. Rad. Transf., 8, 1379

This paper has been typeset from a TEX/ LATEX file prepared by the author.